

IEEE 802.15.4a UWB Receivers' Performance in Different Body Area Network Channels

Ville Niemelä, Matti Hämäläinen, *Senior Member, IEEE*,
Jari Linatti, *Senior Member, IEEE*, Ryuji Kohno, *Senior Member, IEEE*
Centre for Wireless Communications
University of Oulu
Oulu, Finland

E-mail: firstname.lastname@ee.oulu.fi

ABSTRACT

Ultra wideband signals have been first generated in the late 19th century. However, using UWB in data communications increased in popularity since the 1990s. Investigating the effects of human body on the propagation of an UWB signal gained more attention hand in hand with UWB data communications studies. The first studies of human body and UWB signal propagation around it were performed in the early 2000s and ever since the body centric communications have been referred to as body area network. In this paper, we are comparing different UWB receivers capable of detecting the IEEE 802.15.4a format signal in two different UWB WBAN hospital channels; IEEE 802.15.6 CM3 and a real measured and modeled channel.

Keywords

UWB, WBAN, IEEE 802.15.6, IEEE 802.15.4a, channel model, hospital environment, energy detector, rake-receiver,

1. INTRODUCTION

Ultra wideband (UWB) is relatively new research area from data communications perspective. It started to gain more attention in the early 1990s due to an invented impulse radio (IR) UWB device consuming only microwatts of battery power. Before this it had been studied mainly for radar applications. [1-2] Despite the increasing interest in the 1990s of using UWB for data communications, it was not until 2002 when regulations for UWB were first generated by the Federal Communications Commission [3]. Then in 2007, the first global standard on UWB was published by the IEEE, the IEEE 802.15.4a [4]. Now the development is in the phase of creating an UWB standard for wireless body area networks (WBAN) and there will be a new standard, the IEEE 802.15.6, presumably by 2012. Channel model of the IEEE 802.15.6 has already been published in 2009 [5] and it is our interest in this study together with another channel model measured in a real hospital environment.

Ultra wideband has different propagation characteristics compared to the traditional narrow band signals. Therefore extensive studies on UWB channels are well justified and modeling the UWB channels have been widely studied in the recent years. [6-9] Since UWB has very low spectral power density, it is seen as a safe option to be used in many medical applications too. Not to mention that battery life can be very long which, especially in sensor networks, is one of the key feature. One of the challenges of the UWB in medical applications comes from the human body and the signal propagation effects caused by it. The UWB signal is propagating mainly around the human body than through it, as has been spotted in many measurements [7-9]. The body is therefore attenuating the signal and there exist studies showing

that the gender, age and the composition of the body has different impacts on the propagation of UWB signal. [10]

This paper extends and continues the work presented in [11] by reclaiming the future work ideas that were intended to do in it. By simulations, we are evaluating different receivers' performances in two different UWB WBAN channel model. The channel models include the IEEE 802.15.6 channel model 3 (CM3) [5] and a channel model which was measured in a real hospital environment [9]. The latter one was measured in Oulu University Hospital, in Oulu, Finland and was measured by the Centre for Wireless Communications (CWC). It is therefore referred as CWC's channel model. The simulated system model has been implemented based on the IEEE 802.15.4a UWB physical layer definitions. Therefore the receivers are capable of detecting the signal structure defined in [4]. The same simulation model has been used in our earlier work as well [12-14] together with the CWC's channel model [9].

2. SYSTEM MODEL

In the following simulations, a physical layer UWB signal model definitions of the IEEE 802.15.4a standard have been followed. Each of the studied receivers is capable of detecting the aforementioned signal structure. The implementation was performed with Matlab[®]. The transmitted UWB signal and the receiver structures are briefly presented here. For more detailed information about the standard definitions, the reader is referred to the standard itself [4]. In [15] and [16], summaries of the IEEE 802.15.4a standard are provided with analysis. In our earlier work [12-14], the UWB signal and modulation models of the standard are described more detailed too.

The transmitted UWB waveform during the k^{th} symbol interval is expressed as [4]

$$x^{(k)}(t) = [1 - 2g_1^{(k)}] \sum_{n=1}^{N_{\text{cpb}}} [1 - 2s_{n+kN_{\text{cpb}}}] \times p(t - g_0^{(k)}T_{\text{BPM}} - h^{(k)}T_{\text{burst}} - nT_c) \quad (1)$$

where $g_0^{(k)}$ is a position modulated bit and $g_1^{(k)}$ is a phase modulated bit. Sequence $s_{n+kN_{\text{cpb}}} \in \{0,1\}$, $n = 0, 1, \dots, N_{\text{cpb}} - 1$ is the scrambling code used in the k^{th} interval and $h^{(k)}$ is the k^{th} burst hopping position defined also by the scrambler. $p(t)$ is the transmitted pulse waveform at the antenna input, T_{BPM} is the half length of a symbol defining the position of the burst in the symbol, T_{burst} is the length of a burst and T_c is the length of a pulse. [4]

The k^{th} received symbol can be written as

$$r^{(k)}(t) = x^{(k)}(t) * h(t) + n(t), \quad (2)$$

where $x^{(k)}(t)$ is the transmitted signal as in (1), $h(t)$ is the channel impulse response, ‘*’ states convolution and $n(t)$ is a zero mean white Gaussian noise.

There are three receiver types, in which the signal is detected in different ways. These are binary coherent receiver, binary orthogonal non-coherent receiver and energy detector receiver (ED). The first two types can be implemented with rake receivers as the ED presents a simple non-coherent receiver. The different detections are presented below.

Coherent detection is expressed as

$$v_i^{(k)} = \int_q^{q+T_w} r(t - \tau)w(t) d\tau, i = 0,1 \quad (3)$$

where $q = k2T_{\text{BPM}} + iT_{\text{BPM}} + h^{(k)}T_{\text{burst}}$ and T_w being the length of the locally generated reference which is presented as

$$w(t) = \left(\sum_{n=1}^{N_{\text{cpb}}} [1 - 2s_{n+kN_{\text{cpb}}}] \times p(t - nT_c) \right) * h(t) \quad (4)$$

where $h(t)$ is the channel impulse response.

When utilizing the rake receivers, the channel impulse response $h(t)$ is being used by the receiver when generating the reference signal. In selective-rake (s-rake), the n strongest signal component, taps, of the $h(t)$ are utilized and in partial-rake (p-rake) receiver, n first arriving taps are utilized for the same purpose.

In binary orthogonal non-coherent receiver, position modulated binary number is defined by the comparison of the absolute values

$$\left| v_0^{(k)} \right| \begin{matrix} \text{"0"} \\ \geq \\ \text{"1"} \end{matrix} \left| v_1^{(k)} \right|, \quad (5)$$

i.e., if $v_0^{(k)}$ is bigger than $v_1^{(k)}$, the received bit is “0”. Otherwise it is “1”. Note that, since the transmitted signal is also phase modulated, the detection of the position modulated bit is done in a non-coherent manner.

The phase modulated bits are detected by taking the correlation output described in (3) according to the burst position detected by (5). For the larger decision variable v_i ($i = 0$ or 1) from (5), the phase detection is expressed as

$$v_i^{(k)} \begin{matrix} \text{"1"} \\ \geq \\ \text{"0"} \end{matrix} 0. \quad (6)$$

If the correlation output is bigger than zero, the phase detected bit is “1”, otherwise it’s “0”.

The received signal in ED receiver is first passed through a band-pass filter for noise reduction. Assuming that the filter does not cause distortion to the received signal, the decision variable for the position modulation can be written as

$$w_i^{(k)} = \int_q^{q+T_{\text{burst}}+T_{\text{ext}}} r(t)^2 dt, i = 0, 1. \quad (7)$$

In the ED, the integration times are optimized for the channels. T_{burst} is the minimum integration time used by the energy detector. T_{ext} defines the optimized extension of integration time caused by the channel effect.

The decision on the received bit is based on the comparison between the decision variables and it is expressed as

$$w_0^{(k)} \begin{matrix} \text{"0"} \\ \geq \\ \text{"1"} \end{matrix} w_1^{(k)}. \quad (8)$$

Note that, due to the ED receiver structure (7), as the burst length increases, the longer integration time increases also the impact of noise.

3. UWB WBAN CHANNEL MODELS

In the IEEE 802.15.6 channel model report [5], there exist different wireless links for data transmissions. The links, i.e., channel models (CMs) are numbered from 1 to 4. CM 1 is implant to implant, CM 2 implant to body surface, CM 3 body surface to body surface and CM 4 from body surface to external devices with maximum of 5 meter distance. CM 3 is used in this study since it combines both UWB channel model and hospital environment.

Similarly, CWC’s channel models [9] include different on-body links but also different hospital environments, such as a regular hospital room and a surgery room. In the comparisons, the CM 3 and corresponding CWC’s channel model are used. The work of this paper is continuing and extending the work done in [11]. In there, a comparison of the two mentioned channel models was made together with an analysis of the effects.

In this paper, the two channel models are used in the performance simulations of the different receivers capable of detecting the IEEE 802.15.4a UWB signal structure. Due to the incomplete phase of the IEEE 802.15.6 UWB WBAN standard, the previous UWB standard is used.

Table 1 presents a short summary of the main parameters related to the two UWB WBAN channel models. More accurate information on the channel model comparisons can be found in [11]. Detailed channel model information can be found from the original documents of the channel models, [5] and [9].

Table 1. Summarized key parameters of the two channels

	IEEE 802.15.6 CM 3	CWC’s hospital channel model
Average number of arrival paths:	38	over 500
Number of arrival path distribution:	Poisson	Poisson
Mean time difference between consecutive arriving paths:	1.85 ns	0.125 ns
Path amplitude distribution:	Log-normal	Log-normal
Cluster model:	single cluster model	double cluster model

The biggest difference which the used channel models have, relates to the number of resolvable multipath components. In IEEE 802.15.6 CM 3 it is on average 38 as in CWC’s model it is over 500. Another difference is the arriving density in time of the multipath components. In CM 3, the average time difference of the consecutive arriving components is 1.85 ns as in CWC’s model it is 0.125 ns. This is clearly visible in Figure 1, which

shows the normalized channel impulse response of the two used channels. The energy distribution of the channel taps can also see from the Figure 1. It is quite different. In CM 3, the arriving taps are almost evenly distributed in to the time window as in CWC's channel model, the first arriving signal cluster contains the majority of the energy of the taps. This is also the reason why extending the integration time, presented in Figure 2, effects differently on to the ED receiver in different channels.

Common for the two used channel models is that the same SkyCross™ antenna was used in the measurements and that the antenna effect is included in both channel models used.

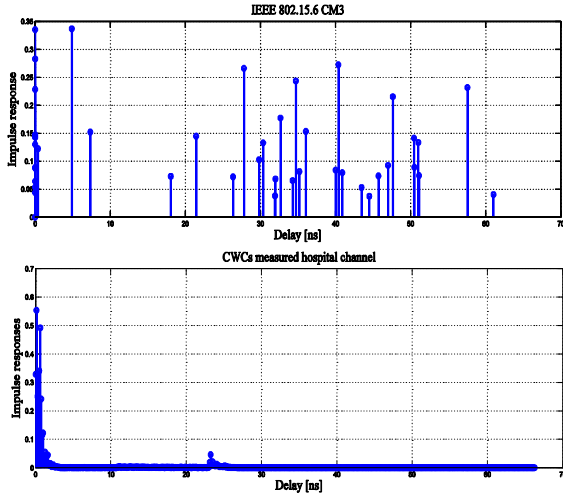


Figure 1. Normalized impulse responses of the two channels.

Figure 2 presents the effect of extending the integration time in the IEEE 802.15.6 CM3. Similar study was performed to the CWC' channel model showing that in it, the extension did not improve the detection performance, or the improvement was insignificant and appeared only with short bursts of two pulses or less. In Figure 2, the resulting bit error rate (BER) curves are with the mandatory mode of the standard IEEE 802.15.4a containing 16 pulses per burst. Three different fixed E_b/N_0 values, 14, 16 and 18 dB are utilized when examining the effect of the extended integration time from the minimum of the length of one burst.

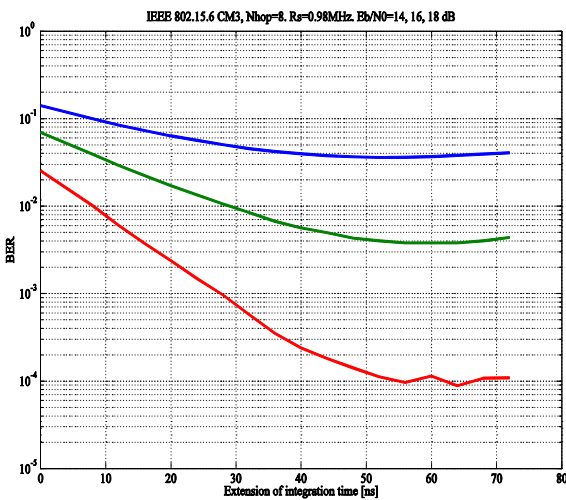


Figure 2. Effect of extending the integration time of the ED.

As can be seen, the improvement of extending the integration time of the ED receiver is quite remarkable when the E_b/N_0 , energy over one burst over zero mean Gaussian noise, is increased. With $E_b/N_0=14$ dB, the extension of the integration time improves BER from 1×10^{-1} to 7×10^{-2} . With $E_b/N_0=18$ dB, the difference in BER is much bigger, from approximately 10^{-2} level to 10^{-4} . The extension in nanoseconds is approximately 50 ns when reaching the saturation level of detection performance and it is not dependent of the used E_b/N_0 values. The extended integration time is quite long when compared to the burst length of 32 ns and when compared to the CWC's channel model in which the extension did not improve the performance at all with the same burst length. The previous section presented the comparison of the two channel models and some answers were found to this phenomenon. In the ED receiver performance evaluation results in Section 4, the optimized extension for each channel is always used.

4. RESULTS

In the performance evaluation, we are using three different detection methods at the receivers. These are binary coherent detection, binary orthogonal non-coherent detection and energy detection. The receiver structures were presented in Section 2. The first two structures can also be executed with either s-rake or p-rake implementation. The used burst length in the presented results is according to the mandatory mode of the IEEE 802.15.4a standard containing 16 pulses per burst and 8 possible burst hopping positions inside one UWB symbol.

Figure 3 presents a performance comparison in BER of p-rake receivers as a function of number of rake fingers. The E_b/N_0 is fixed to 13 dB following the results presented in [13, 14]. The red curves present the benchmark coherent receiver where the position modulated bit is assumed to be known and only the phase modulated bit is detected. This gives a good reference of the best possible performance of a system capable of detecting the IEEE 802.15.4a UWB signal model can have since detecting only the phase modulation performs a binary antipodal demodulation. The black curves present a receiver structure where both position and phase modulated bits are detected. The phase modulated bit is in this case a convolutional channel encoded bit, therefore improving the performance of such receiver. The purple curve presents a performance of a binary orthogonal receiver, where only the position modulated bit is detected as explained in Section 2.

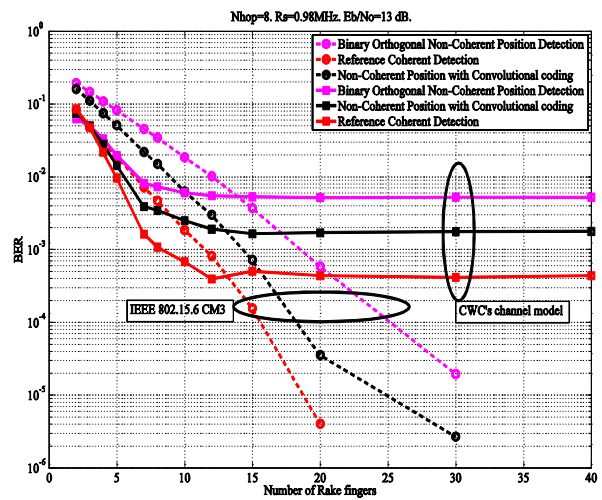


Figure 3. Effect of increasing the number p-rake fingers.

By using different body channel models results in differences in the receiver performances. As can be seen in Figure 3, with p-rake structure of the receivers, there are differences in the performance. If there are less than 13 fingers, the receivers have better performance in CWC's channel than in the CM 3 by the IEEE 802.15.6. The difference is the biggest with around 8 fingers. Then, if the number of fingers is increased, the performance of the receivers are better in CM 3 as in the CWC's model the p-rake receivers reach their saturation level with 10 fingers and with fixed E_b/N_0 of 13 dB. The reason for this can be seen from Figure 1. The energy distribution of the two different channels is very different. In CM3, the amplitudes of the arriving taps remain more or less the same as in CWC's model, the energy of the taps is highly concentrated into the first arriving signal cluster. Therefore, with for example 10 fingers, in CWC's channel, relatively more energy vs. noise is captured than in the CM 3 of the IEEE 802.15.6. Another factor is the big difference in the number of resolvable multipath components of the two channel models, as presented in Table 1. Receiving and processing, for example, 20 taps, results in CM 3 of processing half of the average number of arriving taps as in CWC's model, 20 taps is only 4% of the total number of arriving paths.

In Figure 4, similar receiver performances are presented in BER as a function of E_b/N_0 . Now with s-rake receivers, the number of fingers is kept the same, in 5. With the ED, the optimized extensions for the integration times are utilized.

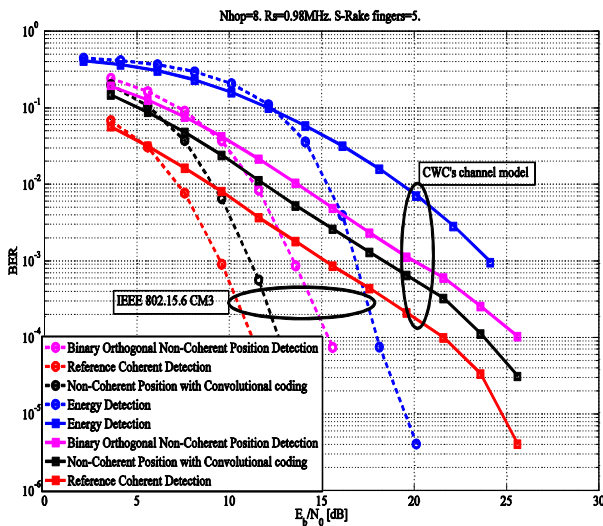


Figure 4. Performance of the ED and s-rake structure receivers.

As can be seen, there exist remarkable differences in the performance of different receivers. Generally, both s-rake receivers with 5 fingers and the ED receiver have better performance in the CM 3 than in the CWC's channel model. For s-rakes, this is due to the fact that collecting five strongest components for the detection contains relatively much more energy in the sparse delay tap channel of CM 3 than in the dense delay tap channel of the CWC.

It is similar situation with the ED. The energy is arriving to the ED in relatively strong portions in the case of CM 3. Even though each noise containing sample is first squared and then integrated, extending the integration time and the integrated noise as well, is not effecting the performance as much as in the case of dense and therefore more scattered CWC's channel.

5. CONCLUSION

Based on our earlier work in [14], the environment is influencing differently, even inside the hospital, on the propagation path of a UWB signal. For achieving better performance and adaptability, low complexity UWB receivers may need to increase the complexity. For example, intelligent rake receivers may switch from n to $n + m$ collected and processed multipaths based on the environment.

As the results and the comparisons here show, there can be quite remarkable differences in two different on-body to on-body UWB channel models. Based on the differences in channel models around human body, adding some intelligence and adaptability to the receivers can be extended here too. I.e., an energy detector could extend the integration time based on the a priori channel information. A priori channel information may be, for example, size, age and gender of the body or when the body is detected moving. Additional to this, the environment is included into the a priori information which can be very useful for the performance of a receiver.

Since different bodies have different characteristics from UWB signal propagation point of view, it may even be impossible to generate one trivial body channel model. Therefore more research on modeling the channel effects of a human body is required. This claim covers different body types and movements of a body as well as human bodies in different environments. At the end of the day, it is very important to have a reliable UWB WBAN channel model which describes and models any given conditions accurately enough, without too much of an uncertainty and controversy.

6. ACKNOWLEDGMENTS

The work for this research has been performed in the projects EWiHS (Enabling future Wireless Healthcare Systems) and it is partly funded by the Finish Funding Agency for Technology and Innovations (TEKES).

7. REFERENCES

- [1] Barret T.W. (2000) History of UltraWideBand (UWB) Radar & Communications: Pioneers and Innovators. *Progress In Electromagnetics Symposium*, PIERS 2000, Cambridge, USA, July, 2000.
- [2] Win M.Z., Dardari D., Molisch A., Wiesbeck W., Zhang J. (2009) History and Applications of UWB. *Proceedings of the IEEE*, Vol. 97, No. 2, pp. 198-204.
- [3] Federal Communications Commission (2002) Revision of Part 15 of the Commission's Rules Regarding Ultra-Wideband Transmission Systems, First Report and Order, 118 p. ET Docket, FCC 02-48, URL: www.fcc.gov, http://fjallfoss.fcc.gov/edocs_public/attachmatch/FCC-02-48A1.pdf, Pages available 8.9.2011.
- [4] IEEE Standard 802.15.4a: Part 15.4: Wireless Medium Access Control (MAC) and Physical Layer (PHY) Specifications for Low-Rate Wireless Personal Area Networks (WPANs), Amendment 1: Add Alternate PHYs. IEEE Computer Society, IEEE Std 802.15.4a-2007 (Amendment to IEEE Std 802.15.4-2006), NY, USA. 187 p.
- [5] IEEE P802.15 Working Group for Wireless Personal Area Networks (WPANs). Channel Model for Body Area Network (BAN). (2009). IEEE 802.15.6 channel modeling subcommittee.

- [6] Molisch A.F., Cassioli D., Chong C-C., Emami S., Fort A., Kannan B. et al. (2006) A Comprehensive Standardized Model for Ultrawideband Propagation Channels. *IEEE Transactions on Antennas and Propagation*, Vol. 54 No. 11. November 2006.
- [7] Zasowski T., Meyer G., Althaus F., Wittneben A (2005). Propagation Effects in UWB Body Area Networks. *IEEE International Conference on Ultra-Wideband*. ICU 2005, Zurich, Switzerland, September 5-8, 2005.
- [8] Fort A., Desset C., Ryckaert J., De Doncker P., Van Biesen L., Wambacq P. (2005) Characterization of the Ultra Wideband Body Area Propagation Channel. *IEEE International Conference on Ultra-Wideband*, ICU 2005, Zurich, Switzerland, September 5-8, 2005.
- [9] Taparugssanagorn, A., Pomalaza-Ráez, C., Isola, A., Tesi, R., Hämäläinen, M., Iinatti, J. (2010) "UWB channel modelling for wireless body area networks in a hospital", *Int. J. Ultra Wideband Communications and Systems*, Vol. 1, No. 4, pp. 226-236.
- [10] Tesi R., Taparugssanagorn A., Hämäläinen M. Iinatti J. (2008). UWB Channel Measurements for Wireless Body Area Networks. *European cooperatipn in the field of scientific and technical research*, COST 2100 TD(08)649, Lille, France, October 6-8, 2008.
- [11] Viittala H., Hämäläinen M., Iinatti J., Taparugssanagorn A. (2009) Different Experimental WBAN Channel Models and IEEE802.15.6 Models: Comparison and Effects. *2nd International Symposium on Applied Sciences in Biomedical and Communication Technologies* (ISABEL 2009), Bratislava, Slovakia, Nov. 24-27, 2009.
- [12] Niemelä V., Rabbachin A., Taparugssanagorn A., Hämäläinen M., Iinatti J. (2010) A Comparison of UWB WBAN Receivers in Different Measured Hospital Environments. *The 3rd International Symposium on Applied Sciences in Biomedical and Communication Technologies*. (ISABEL 2010), Rome, Italy, November 7-10, 2010.
- [13] Niemelä V., Iinatti J., Hämäläinen M., Taparugssanagorn A. (2010) On the Energy Detector, P- and S-Rake Receivers in a Measured UWB Channel Inside a Hospital. *The 3rd International Symposium on Applied Sciences in Biomedical and Communication Technologies*. (ISABEL 2010), Rome, Italy, November 7-10, 2010.
- [14] Niemelä V., Hämäläinen M., Iinatti J., Taparugssanagorn A. (2011) P-Rake Receivers in Different Measured WBAN Hospital Channels. *The 5th International Symposium on Medical Information and Communication Technology* (ISMICT 2011), Motreux, Switzerland, March 27-30, 2011.
- [15] Zhang J., Orlik P.V., Sahinoglu Z., Molisch A.F., Kinney P. (2009) UWB Systems for Wireless Sensor Networks. *Proceedings of the IEEE*. Vol. 97, No. 2, February 2009.
- [16] Karapistoli, E., Pavlidou, F-N., Gragopoulos, I., Tsetsinas, I. (2010) 'An Overview of the IEEE 802.15.4a Standard' *IEEE Communication Magazine*, Vol. 48, Issue 1, pp. 47-53. January 2010.